BUTTERWORTH HEINEMANN

Thermal performance of a pin-fin assembly

R. F. Babus'Haq, K. Akintunde, and S. D. Probert
Department of Applied Energy, Cranfield University, Bedford, UK

The steady-state forced-convective cooling of a horizontally based pin-fin assembly has been investigated experimentally. The circular pin-fins protruded vertically upward from a horizontal base plate. For each in-line or staggered combination of specified pin-fins and air-flow rate, the optimal spacing-to-diameter ratios corresponding to the maximum rate of heat dissipation from the array have been deduced. The effect of changing the thermal conductivity of the pin-fin material has been studied. Designers should aim to have a spacing-to-diameter ratio of 1.04, in the span-wise direction, for all pin-fin systems; whereas, the ratio for the pin-fins in the stream-wise direction will depend upon what fin material is used and whether or not the pin-fins are staggered or aligned.

Keywords: heat transfer; heat exchangers; pin-fins, thermal systems; fluid flow

Introduction

For many industrial applications, internal heat generation can cause serious overheating problems and sometimes leads to system failure. This is especially so in modern electronic systems, in which the packaging density of integrated circuits can be as high as 10^6 chips per square meter (Naik et al. 1987). According to a U.S. Air Force study (Reynell 1990), the four primary sources of stresses that cause failures in avionics systems are temperature (~55%), vibration (20%), excessive humidity (19%), and dust (6%). Humidity is also a temperature-related phenomenon. Therefore, a total of ~74% of breakdowns resulted from thermal overstressing. For example, the temperature of semiconductor components should not exceed the manufacturers' recommendations, typically ~65°C, so that reliable operations can ensue. For a microelectronic device, a 10°C increase above 65°C approximately halves its mean-time-to-failure (Babus'Haq et al. 1992). To overcome this problem, thermal systems with efficient heat sinks (e.g., pin-finned heat exchangers) are essential. Also, optimization of the heat-exchanger design is desirable.

The heat transfer behaviors of pin-films (or full-cross pins) have also been of interest to designers of turbine cooling systems because of their potentially high heat transfer characteristics and surface area density, as well as their structural and castability attributes (Peng 1984). For example, in air-cooled turbine blades, such heat exchangers have made it possible for the blades to be operated at high cycle temperatures, resulting in high specific-power being achieved by modern gas turbines. A review of heat transfer and fluid flow data for arrays of pin-fins in turbine-cooling applications together with appropriate design recommendations is available (Armstrong and Winstanley 1988).

Heat transmissions associated with average flows orthogonal to arrays of long circular cylinders and/or vertical rectangular fins have been investigated extensively (Metzger et al. 1982; Sparrow et al. 1984; Kadle and Sparrow 1986; Leung and Probert 1988; Olson 1992). However, there is a dearth of information concerning the corresponding heat losses from pin-fins. Banks of such fins are arranged usually in either in-line or staggered arrays. The orientation of such systems with respect to the mean flow-direction has a small but possibly significant effect on both the rate of heat transfer and the pressure loss (Metzger et al. 1984; Jurbran et al. 1993; Tahat et al. 1994). The pins' length-to-diameter ratio is the dominant factor influencing the magnitude of array-averaged heat transfer coefficients for short pin-fins (Brigham and VanFossen 1984). However, there is no significant effect for pin height-to-diameter ratios below three; whereas, for ratios greater than three, the array's rate of heat transfer increases with the increasing ratio and approaches that for which long cylinders are used (Armstrong and Winstanley 1988).

The present experimental investigation is aimed at studying the forced-convective thermal-hydraulic characteristics of shrouded pin-fin heat exchangers. The effect of pin-fin spacing, in both the streamwise and the spanwise directions, on the rate of heat dissipation from the heat exchanger for different airflow rates is examined. Optimisation of the geometry of the assembly to obtain maximum rates of heat transfer, while maintaining low viscous losses, is investigated.

Experimental heat transfer rig

Pin-Fin Assembly

The array consisted of circular-section pin-fins (d = 6.35 mm) protruding (H = 190 mm) vertically upward from a 300-mm × 170-mm horizontal rectangular base (see Figure 1). The number of fins is varied in accordance with the fin spacing. For the smallest pin-fin spacing, the maximum number of pin fins is 629; whereas, for the largest spacing, the array consists of only 12 pin-fins. The spacing can be changed from 3.2 mm to 69.6 mm in the spanwise direction and from 1.0 mm to 81.6 mm in the streamwise direction (see Figure 2). The pin-films can be easily removed and replaced with studs made from the same material as the assembly base: when fully screwed in, their heads are flush with the upper surface of the horizontal base plate. Thus, the airflows never flow over a hole in the base plate. The rectangular base as well as the pin-fins were

Address reprint requests to Dr. Babus'Haq at the Dept. of Applied Energy, Cranfield University, Bedford MK43 0AL, UK.

Received 11 April 1994; accepted 12 July 1994

Int. J. Heat and Fluid Flow 16: 50–55, 1995

655 Avenue of the Americas, New York, NY 10010

0142-727X/95/$10.00
SSDI 0142-727X(94)00005-W

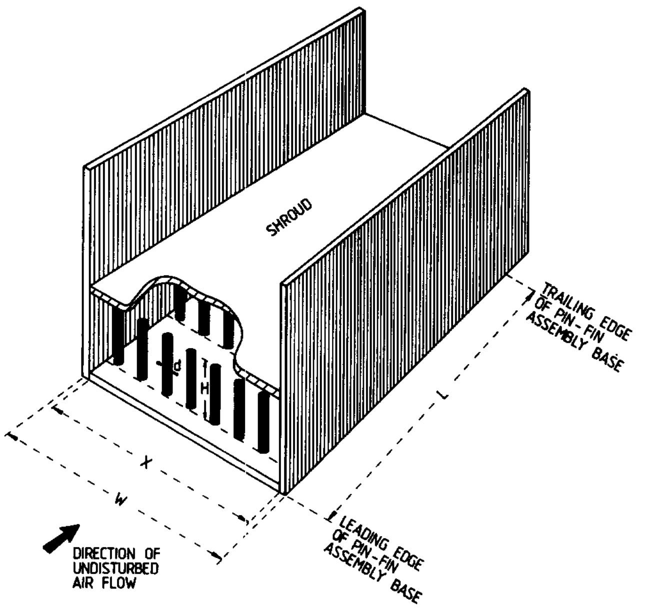

Figure 1 Schematic representation of the shrouded pin-fin assembly

manufactured from light aluminum alloy (i.e., duralumin). Three arrays of pin-fins, manufactured from either duralumin (k = 168 W/mK), mild steel (k = 54 W/mK) or polytetrafluoroethene; i.e., PTFE (k = 1.7 W/mK), were tested. For each test, the pin-fins' height was kept constant with zero clearance between the tips of the pin-fins and the shroud (i.e., they were in full contact with the shroud).

Heating System

The base of the exchanger was heated almost uniformly by four electric-resistor strips, each rated at 500 W: this was the main heater. The base assembly was firmly bolted together, as shown in Figure 3. The presence of thin layers of high thermal-conductivity heat-sink putty ensured that good thermal contact existed between the main heater and the rectangular base, as well as between the fin roots and the rectangular base.

The lower horizontal surface and sides of the main heater block (when operational) were insulated thermally with 80-mm thick mineral-wool blankets. A horizontal guard heater, rated at 500 W, was positioned, parallel to the main heater, below the mineral-wool blanket, with yet another 80-mm layer of mineral-wool placed below it (see Figure 3). The whole system of heat exchanger base, heaters and guard heater, with associated thermal insulation, was located in, and protected by, a well-fitting open-topped wooden box. The horizontal upper

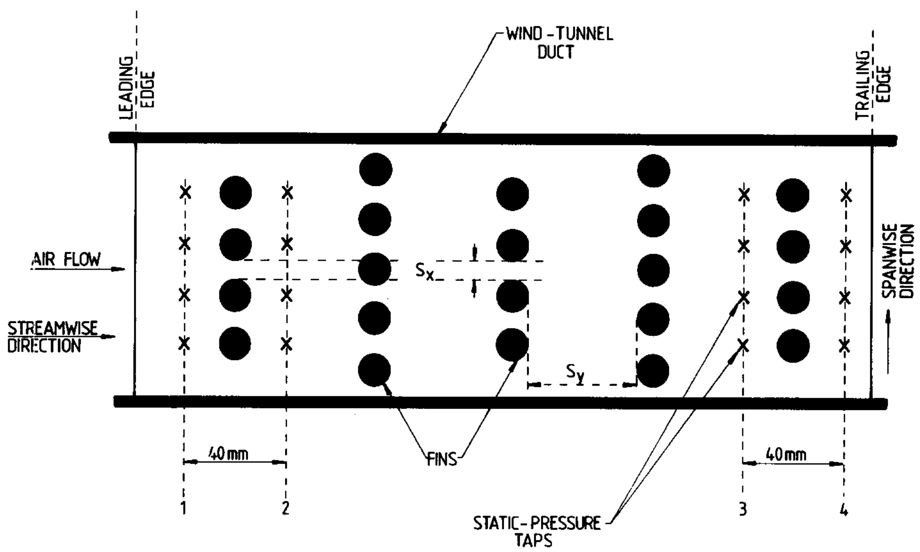

Figure 2 Schematic horizontal-section representation of the locations of the staggered array of pin-fins and the static-pressure taps

Notation

A	area, m^2
d	diameter of each pin-fin (see Figure 1), m
H	vertical protrusion upward of each pin-fin (see Figure 1), m
k	thermal conductivity of the pin-fin material, W/mK
L	length of the pin-fin assembly's horizontal base (see Figure 1), m
p	air pressure, N/m^2
Q	steady-state rate of heat transfer, W
S	separation between adjacent pin-films (see Figure 2), m
T	steady-state temperature, K
V	mean inlet velocity, m/s
W	span-wise external width of the wind tunnel (see Figure 1), m
X	span-wise width of the pin-fin assembly's horizontal base (see Figure 1), m

Subscripts

a	air
b	base of the pin-fin array
opt	optimal
x	span-wise direction
y	stream-wise direction

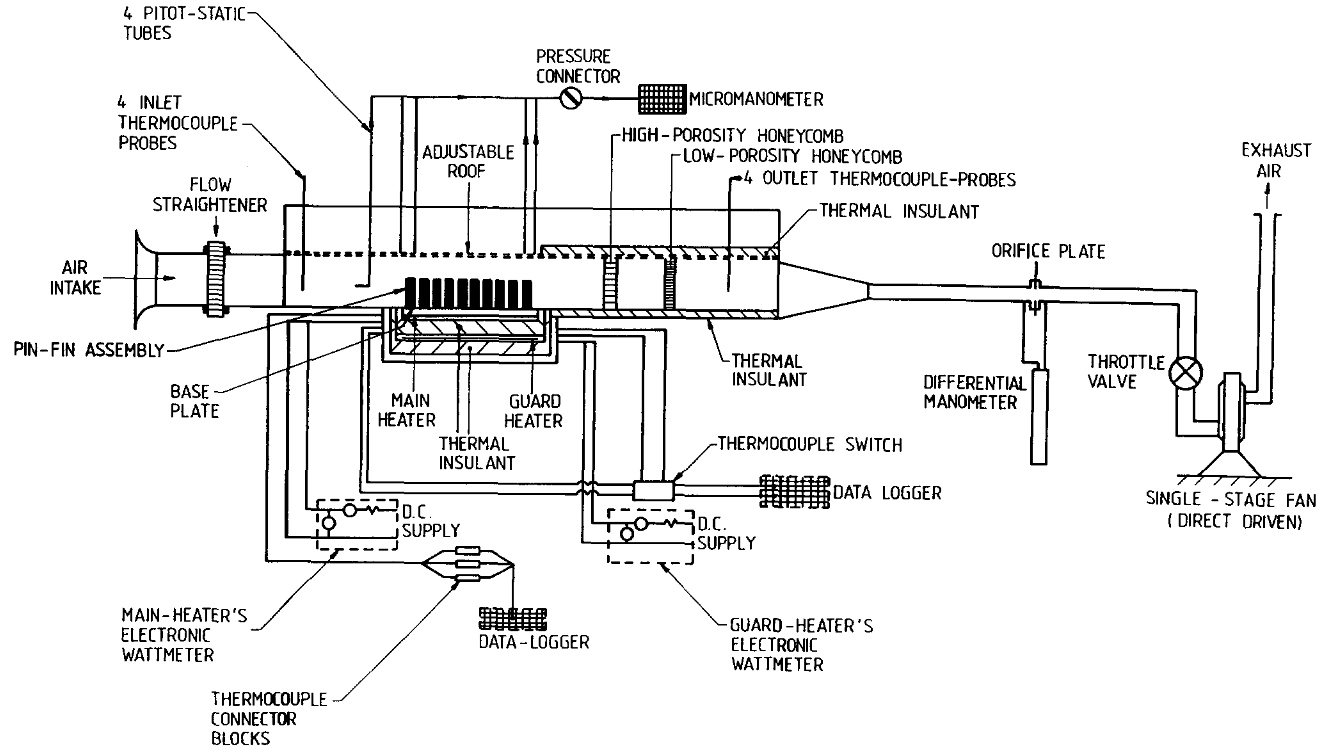

Figure 3 Schematic representation of the experimental rig and the associated instruments

edges of this box and the top surfaces of the laterally-placed thermal insulant during each experiment, were flush with the upper surface of the multi-component rectangular base, from which the fins protruded upward.

The power supplied to the main heater could be adjusted by altering the variac setting and was measured by an in-line electronic Wattmeter. The dissipation in the guard heater was adjusted until the steady-state temperature difference across the layer of insulant, sandwiched between the heaters, was zero. Then, under all the test conditions employed, more than 98 percent of the heat generated in the main heater passed, to the air in the wind-tunnel duct, through the finned heat exchanger. The temperatures at the base of the fin array were indicated by an appropriately distributed set of six copper-constantan thermojunctions embedded within the rectangular base. Each thermojunction was bonded in position with a thin layer of epoxy resin so as to ensure good thermal contact ensued. The average value obtained from these appropriately located thermojunctions was regarded as the mean overall base temperature. This was maintained constant during each experiment at $40 \pm 0.5°C$.

The inlet and the outlet airstream temperatures in the wind-tunnel duct were measured using eight thermocouples: four were located immediately before the entrance of the pin-fin assembly and another four downstream of the array. These could be traversed across the whole inlet and outlet cross sections of the wind-tunnel duct (see Figure 3). All the thermocouples, as well as those indicating the ambient air temperature were connected, through ribbon cables, to a data-logger, which was used to interpret the temperatures, each half hour, until steady-state conditions were attained.

Wind tunnel

The main body of the rectangular cross-sectioned wind-tunnel duct (see Figure 3) was manufactured from wood and was 2-m long with a constant internal width of 240 mm. However, the uniform vertical height of the duct, and hence, the duct's cross-sectional area, could be varied. Different duct heights were obtained by means of an adjustable horizontal roof (or shroud). Approximately halfway along the length of the wind-tunnel duct was the test section. The roof and side walls of this test section were made of 6.35-mm thick Perspex, so enabling the fin array (and the air, via smoke-flow visualization around it) to be observed.

A bell-mouth section was fitted at the entrance of the wind-tunnel duct, followed by a resin-impregnated, low-porosity, cardboard honeycomb flow-straightener. The exhaust air from the pin-fin assembly was passed through an insulated chamber where mixing was accomplished by two resin-impregnated cardboard honeycombs, one being of relatively low porosity and the other of higher porosity. The latter was situated upstream of the former. The two honeycombs were mounted perpendicular to the undisturbed flow stream. At the exhaust end of the duct, a gradual area-contraction section was attached. It was connected, via a plastic pipe, to a single-speed, single-stage fan, and preceded by a throttle control valve. A differential manometer was employed to measure the pressure drop across an orifice plate, which had been calibrated according to BS 1042 (see Figure 3), to indicate airflow speeds.

The wind tunnel was operated in the suction mode; i.e., the fan sucked atmospheric air through the fin assembly and the test section via the bell-mouthed entrance section, with the fan and motor assembly on the exhaust side of the system. This avoided the airstream being heated by the motor prior to its passage through the heat exchanger assembly: this would thereby, have reduced the cooling period capability of the air.

The overall pressure drop through the heat exchanger was obtained via four sets of four static-pressure tappings located in the roof of the test section; i.e., in a plane orthogonal to the direction of the mean airflow (see Figure 2). The velocity profile of the inlet airstream to the fin assembly was obtained via four standard pitot-static tubes. A precise electronic analogue micromanometer was employed to measure the pressure drops.

Measurements uncertainties

In the present investigation, extra care was taken in constructing the heat transfer rig as well as in measuring the temperatures and the electrical power supplied. Each of the stated dimensions was accurate to ± 0.2 mm, and the measured temperatures to $\pm 0.2°C$; whereas, the micromanometer employed to measure the pressures was accurate to ± 0.05-mm water gauge (i.e. ± 0.5 N/m^2) and the Wattmeter to ± 1 Watt.

Observations

The prime objective of a heat exchanger is to transfer the maximum rate of heat with the least amount of energy expended in accomplishing this transfer. The modes of heat transfer from a pin-fin assembly to the surrounding environment are by convection and radiation through the air. The rate of heat transmission depends on the temperatures of the pin-fins as well as the assembly's base; the pin-fins' geometry; the air flow rate; and the orientation of the heat exchanger. Under the considered conditions of the present investigation, the steady-state rate of radiative heat loss from pin-fin assembly with polished surfaces (at just above room temperature) as well as the stray heat loss sideway and downward through the base (i.e., ≤ 5 percent of the total steady-state rate of heat transfer) were considered negligible.

For a constant temperature of the base plate of the pin-fin assembly, the rate of heat transmission can be enhanced by increasing either the heat transfer coefficient, the extended surface area (e.g., by introducing more pin-fins), or both. An increase of the heat transfer coefficient can be achieved if forced (rather than free) convection ensues (e.g., by employing a fan), or changing the geometrical configuration of the heat exchanger. However, the choice is often limited by the pressure drop along the assembly and the resulting rate of energy dissipation.

The pin-fins, beyond the first row of an array, are in the turbulent wakes of the upstream pin-fins. For moderate values of S_y, convection coefficients associated with downstream rows are enhanced by the resulting turbulence of the flow. However, for small values of S_y, upstream rows, in effect, shield downstream rows, and the rate of heat transfer is reduced. That is, the preferred flowpath is in lanes between the pin-fins so much of the pin-fin surface is not exposed to the main flow. For the staggered array, the path of the main flow is more tortuous (compared with those for the in-line array), and a greater portion of the surface area of the downstream pin-fins remains in this path (Incropera and De Witt 1990).

For a fixed configuration of the pin-fin assembly and a consistent uniform spacing of the pin-fins in the stream-wise direction S_y, the steady-state rates of heat transfer were measured for several uniform spacings of the pin-fins in the spanwise direction S_x. Greater rates of heat dissipation from the pin-fin assembly were achieved at higher mean inlet velocities (see Figures 4 and 5 for selected configurations). The optimal spacings were obtained for the three different pin-fin assemblies in the *staggered configuration*. Also, the corresponding optimal spacing-to-diameter ratios were calculated (see Table 1).

It can be seen that, if the pin-fins are chosen to be of the lower thermal conductivity material, the optimal spacing-to-diameter ratio, in the streamwise direction, needs to be

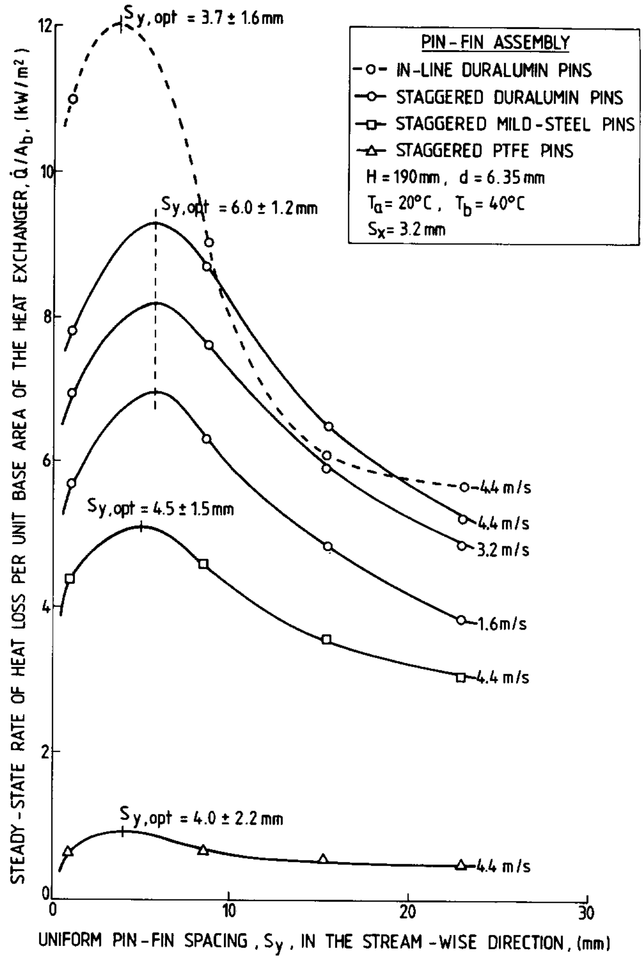

Figure 4 Variations of the steady-state rate of heat loss with the pin-fin spacing in the *streamwise* direction

decreased. For the ranges of the experimental variables tested, a generalized correlation was established: it took the following form:

$$S_{y,opt}/d = 0.59 + 6.67 \times 10^{-2} e^{0.01k} \quad (1)$$

However, for the duralumin pin-fin assembly in the *in-line configuration*, the optimal spacing-to-diameter ratio in the spanwise direction remained invariant at 1.04. Whereas, an optimal value of 0.58 was established in the streamwise direction.

The exhibited curves of Figures 4 and 5 are representative of these obtained for several thousand observations, all indicating qualitatively similar trends to those reported. In order that data at the optimal separations can be established, extra holes for pin-fins on the baseplate are required. However, the existing holes were drilled accurately as close as could be achieved to provide a mechanically robust heat exchanger.

The airflow around the pin-fin array encountered a significant resistance, and hence, an overall pressure drop. However, under similar conditions, this would be higher than that when the pin-fin array is in the in-line configuration (which was less effective for achieving a high rate of heat transfer). Nevertheless, the overall pressure drop decreased, in a similar pattern, as both uniform pin-fin spacings were increased (see Figure 6 for selected configurations).

The results agree qualitatively with those of Jubran et al. (1993) and Tahat et al. (1994) for short pin-fins using an

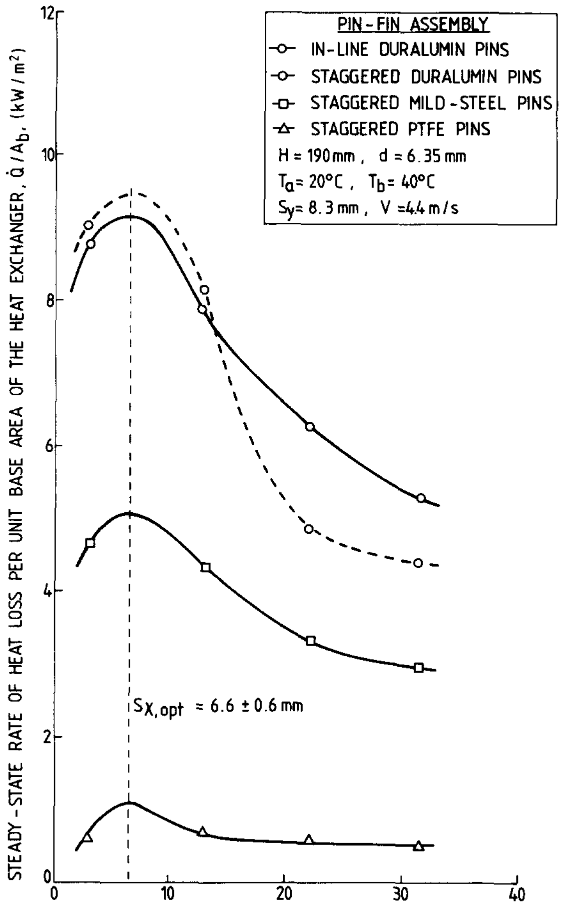

Figure 5 As for Figure 4, but with respect to the pin-fin spacing in the *spanwise* direction

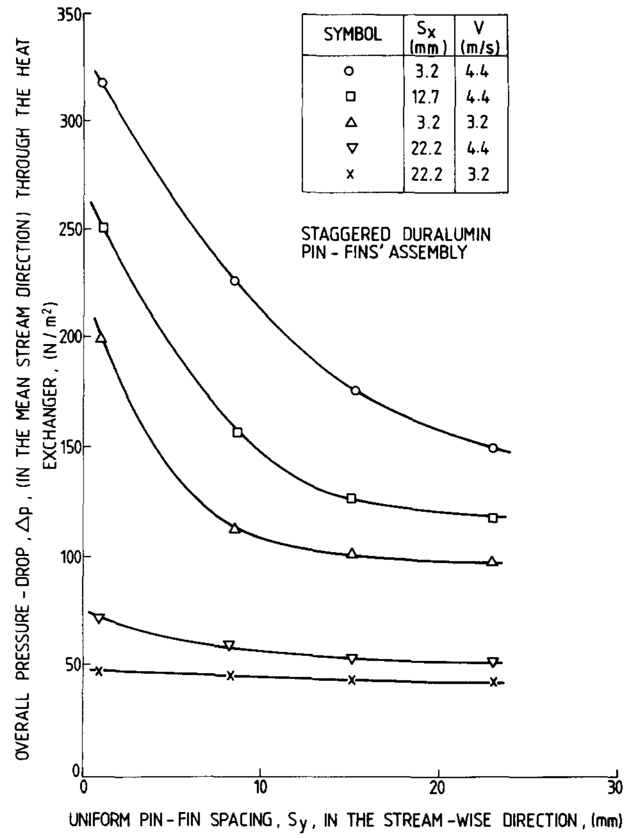

Figure 6 Variations of the overall pressure drop with the pin-fin spacing in the *stream-wise* direction

Table 1 Optimal ratios for the pin-fin assemblies in the staggered configuration

Pin-fin material	$S_{x,\mathrm{opt}}/d$	$S_{y,\mathrm{opt}}/d$
Duralumin	1.04	0.95
Mild-steel	1.04	0.71
PTFE	1.04	0.63

analogous experimental rig, under similar test conditions. However, the optimal spacings in the spanwise and the streamwise directions were 2.5 times the diameter of the pin-fin (Jubran et al. 1993).

Conclusions

The thermal performance of a shrouded vertical duralumin pin-fin assembly in the in-line and staggered configurations has been investigated experimentally. The latter configuration yields a higher steady-state rate of heat transfer than the former configuration, when both are under similar conditions and for equal number of pin-fins.

The optimal separation between the pin-fins in the streamwise direction, corresponding to the maximum rate of steady-state heat transfer from the assembly, increased as the thermal conductivity of the pin-fin material increased: a generalized correlation was obtained; whereas, the optimal separations in the spanwise direction remained invariant.

The overall pressure drop along the heat exchanger for all tested configurations was found to increase steadily with increasing mean inlet velocities and with decreasing uniform pin-fin spacing. The effect of the shroud clearance must be investigated and a heat transmission correlation for assemblies with different pin-fin heights determined.

References

Armstrong, J. and Winstanley, D. 1988. A review of staggered array pin fin heat transfer for turbine cooling applications, *J. Turbomachinery*, **110**, 94–103

Babus'Haq, R. F., George, H. E. and O'Callaghan, P. W. 1992. A thermal-analysis template, *Int. J. Computer Appl. Technol.*, **5**, 67–71

Brigham, B. A. and VanFossen, G. J. 1984. Length to diameter ratio and row number effects in short pin fin heat transfer, *J. Eng. for Gas Turbines and Power*, **106**, 241–245

Incropera, F. P. and DeWitt, D. P. 1990. *Fundamentals of Heat and Mass Transfer*, 3rd. ed., Wiley, New York

Jubran, B. A., Hamdan, M. A. and Abdualh, R. M. 1993. Enhanced heat transfer, missing pin, and optimization for cylindrical pin fin arrays, *J. Heat Transfer*, **115**, 576–583

Kadle, D. S. and Sparrow, E. M. 1986. Numerical and experimental study of turbulent heat transfer and fluid flow in longitudinal fin arrays. *J. Heat Transfer*, **108**, 16–23

Leung, C. W. and Probert, S. D. 1988. Heat-exchanger design: Optimal length of an array of uniformly spaced vertical rectangular fins protruding upwards from a horizontal base, *Appl. Energy*, **30**, 29–35

Metzger, D. E., Berry, R. A. and Bronson, J. P. 1982. Developing heat transfer in rectangular ducts with staggered arrays of short pin fins, *J. Heat Transfer*, **104**, 700–706

Metzger, D. E., Fan, C. S. and Haley, S. W. 1984. Effects of pin shape and array orientation on heat transfer and pressure loss in pin fin arrays, *J. Eng. Gas Turbines and Power*, **106**, 252–257

Naik, S., Probert, S. D. and Shilston, M. J. 1987. Forced-convective steady-state heat transfers from shrouded vertical fin arrays, aligned parallel to an undisturbed air-stream, *Appl. Energy*, **26**, 137–158

Olson, D. A. 1992. Heat transfer in thin, compact heat exchangers with circular, rectangular, or pin-fin flow passages, *J. Heat Transfer*, **114**, 373–382

Peng, Y. 1984. Heat transfer and friction loss characteristics of pin fin cooling configurations, *J. Eng. Gas Turbine and Power*, **106**, 246–251

Reynell, M. 1990. Advanced thermal analysis of packaged electronic systems using computational fluid dynamics techniques, *Computer-Aided Eng. J.*, **7**, 104–106

Sparrow, E. M., Suopys, A. P. and Ansari, M. A. 1984. Effect of inlet, exit, and fin geometry on pin fins situated in a turning flow, *Int. J. Heat Mass Transfer*, **27**, 1039–1054

Tahat, M. A., Babus'Haq, R. F. and Probert, S. D. 1994. Forced steady-state convections from pin-fin arrays, *Appl. Energy*, **48**, 335–351